

Fungi Subvert Vaccine T Cell Priming at the Respiratory Mucosa by Preventing Chemokine-Induced Influx of Inflammatory Monocytes

Marcel Wüthrich,^{1,5,*} Karen Ersland,^{4,5} Thomas Sullivan,¹ Kevin Galles,¹ and Bruce S. Klein^{1,2,3,*}

¹Department of Pediatrics

²Department of Internal Medicine

³Departments of Medical Microbiology and Immunology

⁴The Cell and Molecular Pathology Graduate Training Program

University of Wisconsin School of Medicine and Public Health, Madison, WI 53792, USA

⁵These authors contributed equally to this work

*Correspondence: mwuethri@wisc.edu (M.W.), bsklein@wisc.edu (B.S.K.)

DOI 10.1016/j.immuni.2012.02.015

SUMMARY

Vaccinologists strive to harness immunity at mucosal sites of pathogen entry. We studied respiratory delivery of an attenuated vaccine against *Blastomyces dermatitidis*. We created a T cell receptor transgenic mouse responsive to vaccine yeast and found that mucosal vaccination led to poor T cell activation in the draining nodes and differentiation in the lung. Mucosal vaccination subverted lung T cell priming by inducing matrix metalloproteinase 2 (MMP2), which impaired the action of the chemokine CCL7 on egress of CCR2⁺ Ly6C^{hi} inflammatory monocytes from the bone marrow and their recruitment to the lung. Studies in *Mmp2*^{-/-} mice, or treatment with MMP inhibitor or rCCL7, restored recruitment of Ly6C^{hi} monocytes to the lung and CD4⁺ T cell priming. Mucosal vaccination against fungi and perhaps other respiratory pathogens may require manipulation of host MMPs in order to alter chemokine signals needed to recruit Ly6C^{hi} monocytes and prime T cells at the respiratory mucosa.

INTRODUCTION

The rising rates of systemic fungal infections worldwide have stimulated interest in developing vaccines (Cutler et al., 2007). Although experimental vaccines are under study, none are commercially available (Cutler et al., 2007). An understanding of the mode of action of fungal vaccines will enhance their application in human populations. Th1-cell responses mediated by IL-12 and IFN- γ are believed to foster protective immunity to many pathogenic fungi (Wüthrich et al., 2012). During the earliest stages of fungal infection, pattern recognition receptors on myeloid lineage cells sense fungal pathogens and surfaces (Brown, 2011). Myeloid cells, particularly dendritic cells (DCs), bridge innate and adaptive immunity to pathogens. DCs have thus become a target for vaccine development strategies (Steinman, 2008).

The lung airways of all species are lined with an intraepithelial dendritic network of MHCII^{hi} CD11c^{hi} cells that are mostly CD11b⁻ (Lambrecht and Hammad, 2009). The lamina propria contains MHCII^{hi} CD11c^{hi} cells that express CD11b and elaborate proinflammatory chemokines. CD11b⁺ and CD11b⁻ subsets of DCs express high amounts of CD11c and are viewed as conventional DCs, in contrast to a population of CD11c^{int} plasmacytoid DCs (pDCs). Lung alveoli contain CD11c^{hi} MHCII^{hi} DCs, which are enriched in CD103⁺ subsets. Alveolar macrophages also express CD11c (not CD11b), confusing the analysis of lung DCs unless autofluorescence is used for identifying macrophages (Vermaelen and Pauwels, 2004). Under inflammatory conditions, such as microbial challenge, CD11b⁺ monocyte-derived DCs that rapidly upregulate CD11c and retain Ly6C as a remnant of monocytic descent are recruited (Shi and Pamer, 2011).

Monocyte-derived DCs are important for priming T cell responses to microbes (Hohl et al., 2009; Serbina et al., 2008). These DCs prime Th1 cell responses and IFN- γ -producing Ag-specific CD4⁺ transgenic (tg) T cells in pulmonary aspergillosis (Hohl et al., 2009). In *Aspergillus* infection, CCR2⁺ Ly6C^{hi} DCs are required to prime T cells in the lung, yet not in the spleen. We recently analyzed sequential stages during the induction of vaccine immunity to fungi after subcutaneous (s.c.) injection (Ersland et al., 2010). Monocyte-derived DCs initially take up the most vaccine yeast and traffic them to the skin-draining LNs. However, the direct priming of naive Ag-specific CD4 T cells in vivo is governed by LN-resident DCs and skin-derived DCs. In fact, other skin DCs compensate for monocyte-derived DCs in *Ccr2*^{-/-} mice lacking the cells.

Vaccinologists strive to harness protective immunity at mucosal sites of initial pathogen entry. We sought to immunize against fungal respiratory pathogens by delivering vaccines into the respiratory tract. Although delivery of an attenuated strain of *Blastomyces dermatitidis* (*Bd*) into the skin protects 100% of mice against a lethal pulmonary challenge, and most develop sterilizing immunity (Wüthrich et al., 2000), vaccine delivery intranasally (i.n.) failed to protect and 100% of vaccinees succumbed to infection. Herein, we studied the mechanism behind the failure in priming antifungal vaccine immunity at the respiratory mucosa.

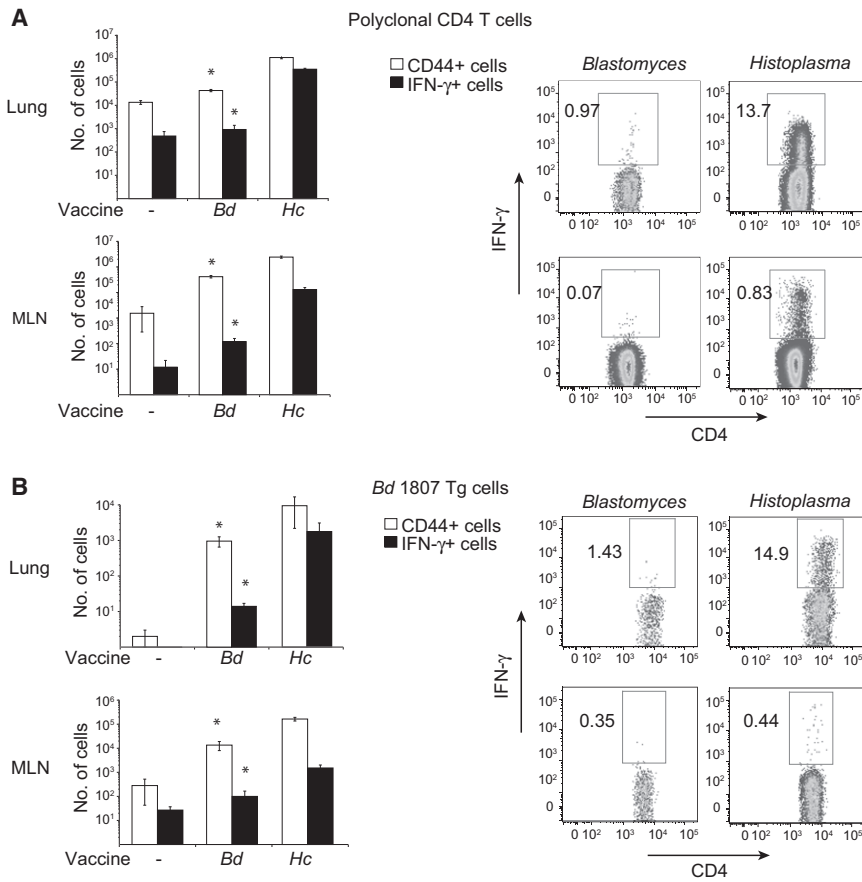


Figure 1. Mucosal Vaccination Induces Poor Th1 Cell Differentiation of Polyclonal and Transgenic CD4⁺ Cells in Response to *Bd*, but Robust Differentiation in Response to *Hc*

Mice were vaccinated with attenuated *Bd* yeast or *Hc* yeast i.t. *p < 0.05 versus mice infected with *Hc*. (A) After i.t. vaccination, cells were harvested from lung 7 days later and stained by FACS to enumerate the number and percentage of activated (CD44⁺) polyclonal CD4⁺ T cells. Lung CD4⁺ T cells were analyzed for intracellular IFN- γ after stimulation with anti-CD3 and -CD28 mAb for 4h. Mean \pm SEM of four mice per group.

(B) After mice received 10⁶ naive 1807 cells i.v., they were vaccinated. *Bd* 1807 cell phenotype and intracellular cytokine were assayed by gating on Th1.1⁺ cells in FACS. Lung cells were harvested 7 days after i.t. vaccination. Dot plots show the percentage of IFN- γ ⁺ Thy1.1⁺ CD4⁺ 1807 cells after stimulation with anti-CD3 and -CD28 mAb for 4 hr. Cells from the MLN were harvested 7 days after vaccination and stained so that the number and percentage of activated (CD44⁺) Thy1.1⁺ CD4⁺ T cells could be assayed. T cells were stimulated with CW/M antigen for 16 hr and stained for IFN- γ . Mean \pm SEM of four mice per group.

(Wüthrich et al., 2000) or intratracheally (i.t.) (data not shown) were unable to control infection and died after pulmonary challenge. This scenario contrasts with that for *Histoplasma capsulatum* (*Hc*), in

We report that fungi subvert the induction of vaccine immunity at the respiratory mucosa by inducing lung matrix metalloproteinase 2 (MMP2), which suppresses the action of CCL7 and impairs recruitment and maturation of Ly6C^{hi} inflammatory monocyte-derived DCs in the lung. Elimination of mature Ly6C^{hi} DCs at this site retarded the activation, expansion, and differentiation of IFN- γ ⁺ CD4⁺ T cells. Conversely, administering an MMP2 inhibitor or CCL7 during vaccine delivery restored recruitment of Ly6C^{hi} monocytes to the lung and priming of CD4⁺ T cells. Our results pinpoint mechanisms that underpin vaccination against fungi at the respiratory mucosa. They also highlight host and microbial strategies that must be overcome to engineer fungal and other vaccines that induce respiratory mucosal immunity. Mucosal vaccination against respiratory agents may require manipulation of host MMPs that alter chemokine signals needed to recruit Ly6C^{hi} inflammatory monocytes and prime CD4⁺ T cells at the respiratory mucosa.

RESULTS

Fungal Vaccination at the Respiratory Mucosa

Subcutaneous injection of mice with a live attenuated *Bd* strain engenders 100% survival against a lethal pulmonary challenge (Wüthrich et al., 2000), but inconsistent sterilizing immunity. Because the natural route of infection is inhalation of spores, we sought to enhance the vaccine's efficacy by delivering it into the respiratory tract. All mice vaccinated intranasal (i.n.)

which primary pulmonary infection induces protective immunity and resistance against lethal pulmonary challenge (Deepe and Seder, 1998). Because these two fungal infections require cellular immunity for resistance, we compared the priming of CD4⁺ T cells for each of them to uncover the reasons for failure versus success in priming of T cells at the respiratory mucosa.

Th1 cell differentiation occurs fully after CD4⁺ T cells migrate to the lung (Rivera et al., 2006). Although i.t. vaccination with *Bd* induced activated CD4⁺ T cells (CD44⁺) cells in the lung, Th1 cells failed to accrue and <1% produced IFN- γ (Figure 1A). There were \approx 1,000-fold less IFN- γ ⁺ CD4 T cells in the lung after i.t. vaccination with *Bd* compared with *Hc*. *Hc* induced a 1,000-fold increase in the number of IFN- γ ⁺ CD4 T cells in the lung upon mucosal vaccination, with nearly 14% producing IFN- γ , whereas *Bd* induced little increase. In contrast, s.c. administration of *Bd*, as well as *Hc*, lead to marked expansion of IFN- γ ⁺ cells during a recall response after challenge. Mice given *Bd* s.c. had 100-fold more IFN- γ ⁺ cells than unvaccinated controls, and more than 7% of CD4⁺ T cells produced this cytokine (Figure S1A available online).

Several mechanisms could explain the small number of IFN- γ ⁺ cells and the inability of attenuated *Bd* to vaccinate at the respiratory mucosa. First, the vaccine may not induce proliferation of *Bd* specific CD4⁺ T cells or promote their survival. Second it may not induce differentiation of Ag-specific T cells. Third, Th1 CD4⁺ T cells may not be recruited from MLN into the lung airways. Last, CD4 T cells may not fully

differentiate or mature into Th1 cells in the lung. To distinguish among these possibilities, and interrogate T cell priming, expansion, differentiation and trafficking, we generated a TCR tg mouse specific for *Bd*.

Generation and Characterization of a TCR tg Mouse

The *Bd* 1807 TCR tg mouse was engineered (Figures S1C–S1F; see Supplemental Experimental Procedures) from a CD4⁺ T cell clone that confers protective immunity against lethal pulmonary challenge in mice (Wüthrich et al., 2007). *Bd* 1807 mice have an increased prevalence of V α 2⁺ CD4⁺ T cells in the peripheral blood, spleen, and LNs versus wild-type B6 mice (Figure S1E). Naive CD4⁺ T cells from *Bd* 1807 mice became activated and proliferated in response to cell wall-membrane antigen (CW/M), whereas CD4⁺ T cells from naive wild-type mice did not respond to CW/M (Figure S1F). Thus, *Bd* 1807 cells are specific and responsive to *Bd* *in vitro*.

Bd 1807 cells respond to *Bd* and cross-react with *Hc* after s.c. vaccination (Wüthrich et al., 2011b), they become activated in the draining LNs, differentiate into Th1 effector cells on migration to the vaccine site, and exhibit memory and recall to lung upon lethal pulmonary infection. *Bd* 1807 cells not only show fidelity with polyclonal CD4⁺ T cells, but they also report the behavior of CD4⁺ T cells that confer protective immunity (Wüthrich et al., 2007). Thus, *Bd* 1807 cells enable interrogation of CD4⁺ T cell priming, expansion and trafficking in response to both fungi, and comparisons of these events between them.

Disparate Vaccine Priming of *Bd* 1807 Cells by *Bd* versus *Hc* at the Respiratory Mucosa

We compared the priming of *Bd* 1807 tg CD4⁺ T cells in response to vaccination with *Bd* or *Hc* in the lung. Although *Bd* 1807 cells respond vigorously to both fungi after vaccination s.c. (above), when vaccine is instead given i.t., the activation, expansion, and differentiation into IFN- γ effector cells is sharply reduced in mice given *Bd* versus *Hc* (Figure 1B). The discrepancies between the two groups were most exaggerated for IFN- γ ⁺ 1807 cells in the lung. *Hc*-vaccinated mice had >100-fold more 1807 Th1 effector cells compared to *Bd*. In lung-draining or mediastinal LNs (MLN), *Bd*-vaccinated mice also had 10- to 100-fold fewer activated cells. In contrast, after s.c. vaccine, *Bd* 1807 cells were activated (CD44⁺) in the sLNs efficiently in response to both fungi, and similar numbers of antigen-specific IFN- γ ⁺ T1 effector cells were recalled to the lung (Figure S1B).

Thus, *Bd* 1807 cells let us pinpoint defects in priming CD4⁺ T cells after delivery of *Bd* vaccine in the lung, which are linked to (1) impaired activation and expansion in the lung-draining MLN and (2) profound failure to differentiate fully into Th1 IFN- γ -producing effector cells upon migration back to lung after mucosal vaccination. These deficits probably underpin failed vaccination by *Bd* at the respiratory mucosa. The results contrast sharply with the robust priming, expansion, and differentiation of *Bd* 1807 cells in response to *Hc* delivered via the respiratory route and to *Bd* vaccine delivered by the s.c. route. These differences raise the question: why does *Bd* vaccine fail to prime T cells at the respiratory mucosa and what mechanism accounts for the sharp disparity in vaccine priming in the lung by these two closely related fungi?

Recruitment of Ly6C^{hi} Inflammatory Monocytes upon Mucosal Vaccination

We analyzed the myeloid APCs recruited to the lung after delivery of vaccine yeast into the respiratory tract. We looked at CD103⁺ DCs, CD11b⁺ DCs, including inflammatory monocyte-derived Ly6C^{hi} DCs, alveolar macrophages, and neutrophils. We saw sharp differences in the influx of APCs and uptake of yeast for the two fungi. CD11b⁺ DCs were among the most prominent APCs recruited to the lungs by both fungi (Figures 2A and S2C–S2F). The sharpest difference between the two fungi was in the influx of Ly6C^{hi} CD11b^{hi} cells. Ly6C^{hi} monocytes accounted for \approx 10% of the lung cells in response to *Hc* versus <1% for *Bd* (Figure 2B). By staining yeast with PKH26, we honed in on lung APC that harbored yeast (Figures 2C, 2D, and S2D–S2F). CD103⁺ DCs contained few yeast (Figure 3C). In contrast, for both fungi, most yeast resided with CD11b⁺ DCs (Figures 2C and S2D) and also in macrophages and neutrophils (Figures S2E and S2F). Strikingly, there were >10-fold more Ly6C^{hi} CD11b^{hi} cells in the lung harboring *Hc* versus *Bd* (Figures 2C and 2D).

The same disparity between these fungi was seen in the draining MLN (Figures 2E–2H). Ly6C^{hi} CD11b^{hi} cells were nearly absent in the MLN of *Bd*-vaccinated mice (0.045%), whereas the proportion of these cells in the MLN of *Hc*-vaccinated mice was 30-fold higher (1.4%) (Figures 2E and 2F). Most of the DCs that harbored yeast in MLN were CD11b⁺ DCs, although some CD103⁺ cells also harbored yeast for both fungi (Figure 2G). Still, the biggest difference between the two fungi was again in Ly6C^{hi} CD11b⁺ cells; the proportion of these cells harboring *Hc* (7.2%) was \approx 12-fold higher than that for *Bd* (0.59%) (Figure 2G). Consequently, in the MLN, there were >1000-fold more Ly6C^{hi} inflammatory monocytes with *Hc* ($\geq 10^3$ cells) than *Bd* (≤ 10 cells) (Figure 2H). Thus, the numbers of Ly6C^{hi} monocytes that are recruited to the lung and migrate into the draining MLN, and the numbers of these DCs harboring yeast, are sharply reduced in mice that received *Bd* compared to *Hc*.

Bd Blocks the Recruitment of Ly6C^{hi} Inflammatory Monocytes to the Lung

The blunted entry of Ly6C^{hi} monocytes into the lungs of *Bd*-vaccinated mice could be due to either a failure to induce the recruitment of these cells or, alternatively, an active process of blocking their recruitment. To distinguish between the two possibilities, we performed a mixing experiment in which we added *Bd* vaccine yeast to the inoculum of *Hc* given i.t. The addition of *Bd* curtailed the recruitment of Ly6C^{hi} monocytes into the lung by *Hc* (Figure 3A). In the mixed infection, the distribution and numbers of DCs showed a paucity of Ly6C^{hi} CD11b⁺ DCs (0.26%) that was similar to mice vaccinated with *Bd* (0.19%) and much lower than mice that received *Hc* (13.7%) (Figure 3A); the numbers of total Ly6C^{hi} DCs in the lung followed similar trends with almost identical patterns for *Bd* and mixed infections, each much lower than for *Hc* vaccination (Figure 3B). To see whether mixed infection perturbed the numbers of APC harboring yeast, we stained the yeast with PKH26. The total number of yeast-loaded APCs in the lung was increased in the mixed infection (Figure S3B), although the numbers of Ly6C^{hi} (and Ly6C^{hi} CD11c⁺) cells that harbored yeast was greatly reduced in the mixed-infection and

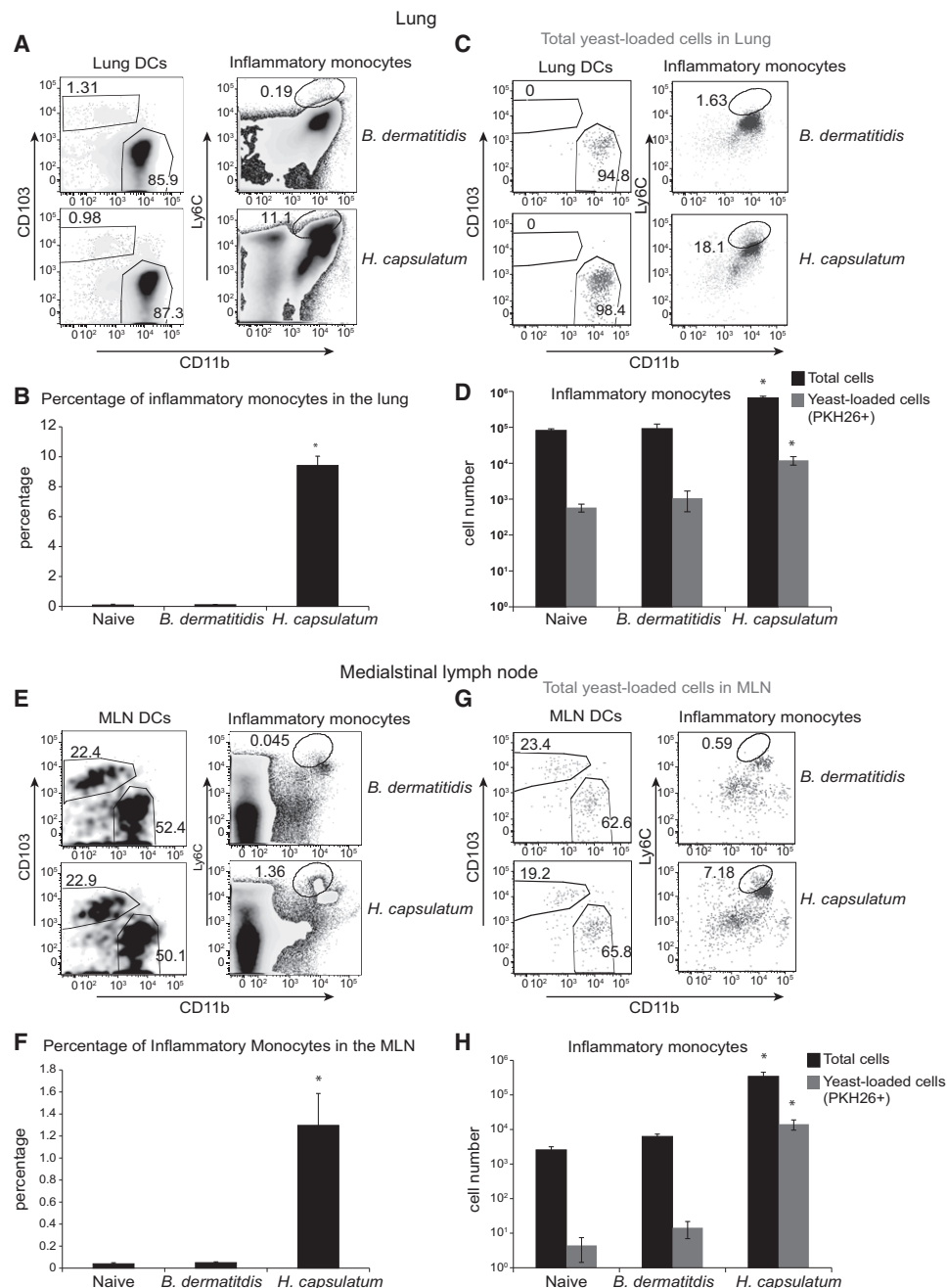


Figure 2. Inflammatory Monocytes Are Recruited to the Lung in Response to *Hc* but Not *Bd*

(A) Mice received 10^5 attenuated *Bd* yeast or 10^6 *Hc* yeast i.t. Lungs were harvested 4 days after infection, digested with collagenase D, and stained for flow cytometry. Cells were initially gated on FCS/SSC and then underwent live cell gating, based on fixable live/dead staining. Left column shows the phenotype of lung DCs (MHCII⁺ CD11c⁺ cells) that stain positive for CD103 and CD11b. Right column shows the inflammatory monocytes in the lung characterized by Ly6C and CD11b expression, indicated in the circled gate.

(B) Percentage of lung cells that are inflammatory monocytes after exposure to the fungi. Gate for percentages are shown in Figure 2A. * $p < 0.05$ versus respective sample for *Bd* group. Error bars represent the mean \pm SD of four mice per group. Data are representative of five independent experiments.

(C) The phenotype of lung cells containing PKH26⁺ yeast were identified as in (A).

(D) Number of total (black bars) and yeast-loaded (PKH26⁺) inflammatory monocyte (red bars) in the lung. Gate for percentages are shown in Figure 2C. Numbers were calculated based upon FACS percentages and cell counts. * $p < .05$ versus respective sample in *Bd* group. Error bars represent the mean \pm SD of four mice per group. Data are representative of five independent experiments.

(E–H) Characterization of cells in the draining MLNs of mice that received fungi as above; MLNs are harvested at the same time as the lungs. Data from the MLNs is depicted as in (A)–(D), respectively. * $p < .05$ versus the respective sample for the *Bd* group.

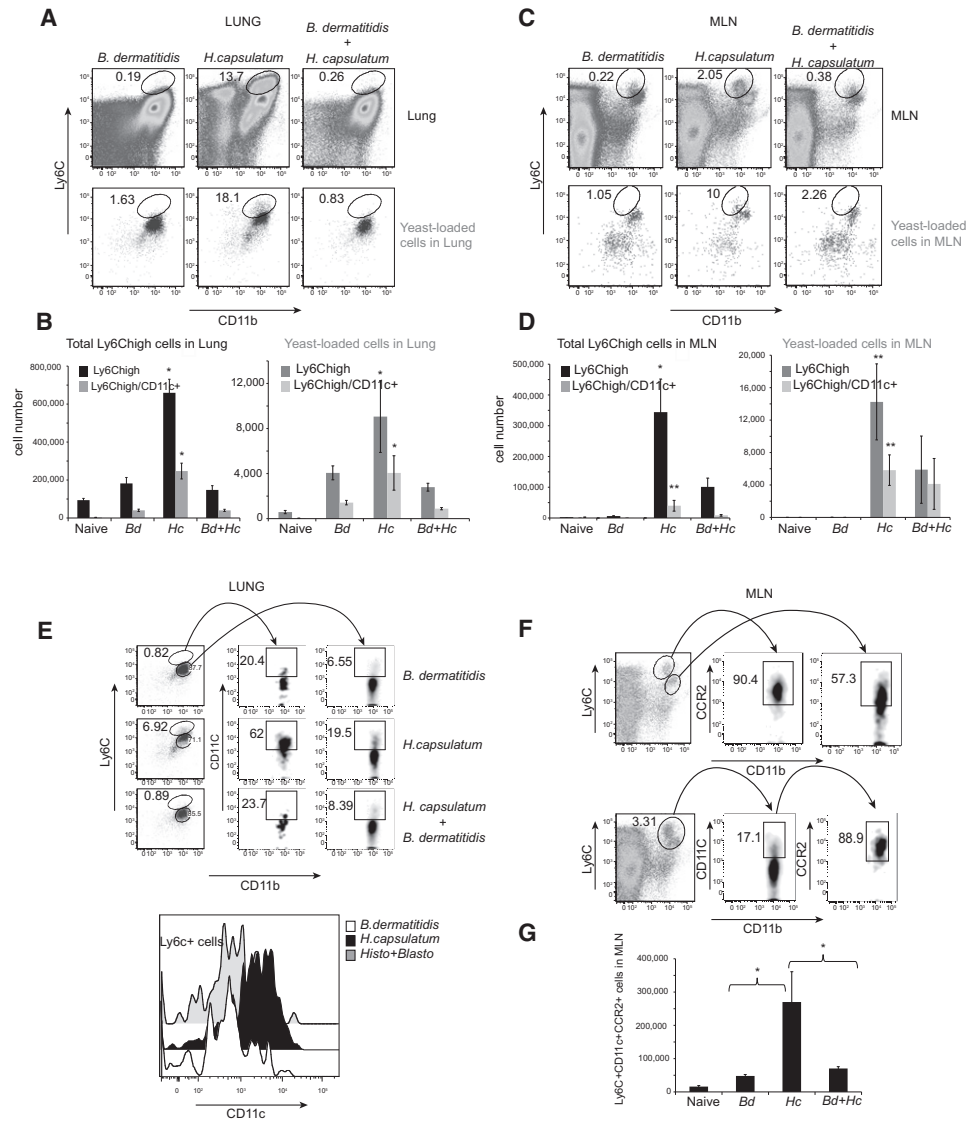


Figure 3. *Bd* Retards the Influx and Maturation of Inflammatory Monocytes in the Lung

(A) Inflammatory monocyte phenotype in the lungs of mice that received 10^5 *Bd*, 10^6 *Hc*, or a mixture of yeast i.t. Gates in the top row depict the percentage of inflammatory monocytes among total lung cells; gates in the bottom row show the percentage of inflammatory monocytes among lung cells containing PKH26⁺ yeast.

(B) Numbers of total Ly6C^{hi} monocytes (black bars) and total Ly6C^{hi} CD11c⁺ cells (gray bars) 4 days after mice received yeast i.t.. * $p < 0.05$ for *Hc* group versus *Bd* alone- or mixed-fungal group. The numbers of yeast-loaded (PKH26⁺) Ly6C^{hi} monocytes (red bars) and PKH26⁺ Ly6C^{hi} CD11c⁺ cells (pink bars) 4 days after mice received yeast i.t.. * $p < 0.05$ for *Hc* group versus *Bd* alone- or mixed-fungal group.

(C) Phenotype of inflammatory monocytes in MLN (top row) and of cells containing PKH26⁺ yeast (bottom row).

(D) Numbers of total Ly6C^{hi} monocytes (black bars) and total Ly6C^{hi} CD11c⁺ cells (gray bars) in the draining MLNs 4 days after mice received fungi i.t.. * $p < 0.05$ for *Hc* group versus *Bd* alone- or mixed-fungal group. ** $p < 0.05$ for *Hc* group versus *Bd* group. Number of yeast-loaded (PKH26⁺) Ly6C^{hi} monocytes (red bars) and PKH26⁺ Ly6C^{hi} CD11c⁺ cells (pink bars) in the MLN 4 days after mice received fungi i.t.. * $p < 0.05$ for *Hc* group versus *Bd* alone- or mixed-fungal group. ** $p < 0.05$ for *Hc* group versus *Bd* group.

(E) CD11c expression of PKH26⁺ Ly6C^{hi} (middle row) and PKH26⁺ Ly6C⁺ (right row) cells in the lung of mice that received i.t. inoculation of *Bd*, *Hc*, or the two yeast mixed. Arrow denotes the CD11c expression of the population indicated. Histogram of CD11c expression on PKH26⁺ Ly6C⁺ cells (the gate was drawn to include both Ly6C^{hi} and Ly6C⁺ cells) from mice that received i.t. inoculation of *Bd* (white), *Hc* (black), or the two yeast mixed (gray).

(F) CCR2 expression on Ly6C^{hi} and Ly6C⁺ cells in the draining MLNs of mice 4 days after they received i.t. inoculation *Hc* (top row). The bottom row shows CCR2 expression on Ly6C⁺ CD11c⁺ cells in mice that received i.t. inoculation of *Hc*.

(G) Absolute number of Ly6C⁺ CD11c⁺ CCR2⁺ cells in the draining MLNs of mice that received i.t. inocula of *Bd*, *Hc*, or both yeast mixed together. Numbers are derived from percentages based on flow analysis. * $p < 0.05$ for comparisons indicated in brackets. Error bars in (B), (D), and (G) represent the mean \pm SD of four to five mice pre group and the data are representative of three independent experiments.

Bd-alone groups, as compared to the *H. capsulatum* group (Figure 3B). The patterns in the MLN mirrored those in the lung (Figures 3C and 3D). Thus, *Bd* interferes with either recruitment or entry and migration of Ly6C^{hi} monocytes in the lung and MLN and can do so even in the case of a strong inducing stimulus like respiratory exposure to *Hc*.

Ly6C^{hi} monocytes that enter the lung in response to infection mature upon transition to DCs, involving downregulation of Ly6C and upregulation of CD11c and MHC class II (Osterholzer et al., 2009). We explored this process in the three groups: either yeast alone or mixed together. For Ly6C^{hi} monocytes that entered the lung in response to mucosal vaccination with *Bd*, both the Ly6C expression and the CD11c expression were much lower than that compared to the *Hc* group, and the mixed infection yielded a pattern similar to that for *Bd* alone (Figure 3E). Thus, in the setting of *Bd* vaccine, low Ly6C expression was not due to the maturation to CD11c⁺ DCs; the yeast instead blunted the maturation of CD11cDCs.

Ly6C^{hi} inflammatory monocytes trafficking to organs may require CCR2 expression (Serbina et al., 2008). Over 90% of the Ly6C^{hi} monocytes that migrate into the MLNs in response to *Hc* display CCR2 (Figure 3F). Among the CD11c⁺ Ly6C⁺ cell population in the MLN in this setting, 90% express CCR2. Importantly, Ly6C^{hi} CD11c⁺ CCR2⁺ cells numbered ≈5-fold more after the mucosal delivery of *Hc*, compared to *Bd* or mixed infection (Figure 3G).

Mucosal Vaccination with *Bd* Retards Chemokine Action, Blocking Egress of Ly6C^{hi} Inflammatory Monocytes from the Bone Marrow and Recruitment into the Lung

We investigated mechanisms behind the impaired influx of Ly6C^{hi} inflammatory monocytes upon respiratory vaccination with *Bd*. CCR2⁺ inflammatory monocytes emanate from the bone marrow in response to chemokine signals, so we first analyzed whether the defect in cell recruitment is due to failed egress of cells from the bone marrow or failed entry into the lung. In wild-type mice, the percentage of Ly6C^{hi} monocytes in the marrow was ≈2-fold higher in animals that got *Bd* or mixed infection, compared to *Hc* (Figure 4A). This increase could be due to trapping of cells in the marrow or increased production. To distinguish these possibilities, we studied *Ccr2*^{-/-} mice in which these cells cannot exit the marrow (Serbina and Pamer, 2006). Production is increased in the *Hc* group relative to the other groups (Figure S4A), suggesting that overproduction does not explain the accumulation for *Bd* relative to *Hc* in wild-type mice. We did not see a difference between groups in the number of circulating monocytes during 2–5 days after vaccination (data not shown). Thus, mucosal delivery of *Bd* leads to failure of egress and trapping of Ly6C^{hi} monocytes in the marrow rather than defective monocyte extravasation into the lung.

The major signals that induce egress of CCR2⁺ monocytes from the bone marrow are CCL2 and CCL7 (Jia et al., 2008; Tsou et al., 2007). To see whether *Bd* affected these chemokines, we analyzed levels in the lungs and serum of mice from the three groups. The most striking difference was elevated serum levels of CCL7 in those that received *Bd* i.t. (Figure 4B). We tested the activity of these sera in promoting migration of Ly6C^{hi} monocytes in vitro. Sera from mice that got *Hc* promoted

the migration of Ly6C^{hi} monocytes, whereas sera from the *Bd* group did not (Figure 4C). Thus, the elevated levels of CCL7 in *Bd* sera failed to induce chemotaxis.

Chemokines can be inactivated by serine proteases of mammalian or microbial origin. To test whether inactive CCL7 might explain the defects in bone marrow egress of *Bd*-vaccinated mice, we vaccinated the mice together with recombinant CCL7. Recombinant CCL7 given to *Bd*-vaccinated mice enhanced the egress of Ly6C^{hi} monocytes out of the marrow and induced their recruitment into the lungs (Figure 4D). Thus, the elevated endogenous levels of CCL7 in serum were not functional in vivo.

Inactive chemokines can desensitize their receptor (Ali et al., 2005). We studied the migration of bone marrow monocytes in vitro in response to both CCL7 and CCL2. Ly6C^{hi} monocytes from naive mice showed a ≈3-fold increase in migration toward these chemokines compared to medium alone, whereas cells from *Bd*-vaccinated mice showed significantly less migration toward the ligands (Figure S4B). We further analyzed receptor desensitization by measuring Ca²⁺ flux. The flux of bone marrow Ly6C^{hi} monocytes in response to CCL7 as well as CCL2 is curtailed in cells from *Bd*-vaccinated mice compared to naive mice (Figure 4E; data not shown). Thus, Ly6C^{hi} monocytes from *Bd*-vaccinated mice showed reduced sensitivity to their ligands, promoting their trapping in the marrow and poor recruitment to the lung.

Mammalian Lung MMP2 Is Induced by Fungal Vaccination at the Respiratory Mucosa

Chemokines can be inactivated by mammalian MMPs. The gelatinase MMP2 acts on CCL7 converting it into an inactive or antagonistic form (McQuibban et al., 2000; McQuibban et al., 2002). We investigated lung MMP2 in response to vaccination at the respiratory mucosa. The level of active MMP2 in bronchoalveolar lavage (BAL) fluid was several-fold higher in mice vaccinated with *Bd* versus *Hc* (Figure 5A). To see whether the MMP2 levels affected chemokine-mediated egress of Ly6C^{hi} monocytes from the marrow to the lung, we inhibited MMPs during vaccine administration. The broad MMP inhibitor, GM6001, and the MMP2-selective inhibitor promoted egress of Ly6C^{hi} monocytes from the bone marrow (Figure S5A) and increased their recruitment to the lung in mice vaccinated i.t. with *Bd* (Figure 5B). These inhibitors did not affect the growth of the fungus in the lung (data not shown). Vaccination of *Mmp2*^{-/-} mice also augmented the release of Ly6C^{hi} monocytes from the marrow (Figure S5B) and influx of these cells into the lung compared to vaccinated wild-type mice (Figure 5C). Thus, induction of lung MMP2 and inactive CCL7 underpin the trapping of Ly6C^{hi} monocytes in the bone marrow and their failure to traffic to the lung in response to fungal vaccine administration at the respiratory mucosa.

Ly6C^{hi} CD11b⁺ CCR2⁺ Cells and Vaccine Priming of *Bd* 1807 Cells at the Respiratory Mucosa

We examined how impaired influx of Ly6C⁺ CD11b⁺ CD11c⁺ CCR2⁺ cells upon vaccination affects priming of protective CD4⁺ T cells in the lung, including *Bd* 1807 cells. We used *Ccr2*^{-/-} mice to establish the contribution of Ly6C^{hi} monocytes (Figure 6A). Expansion of *Bd* 1807 cells in the MLN was markedly impaired in wild-type mice that received *Bd* or mixed infection

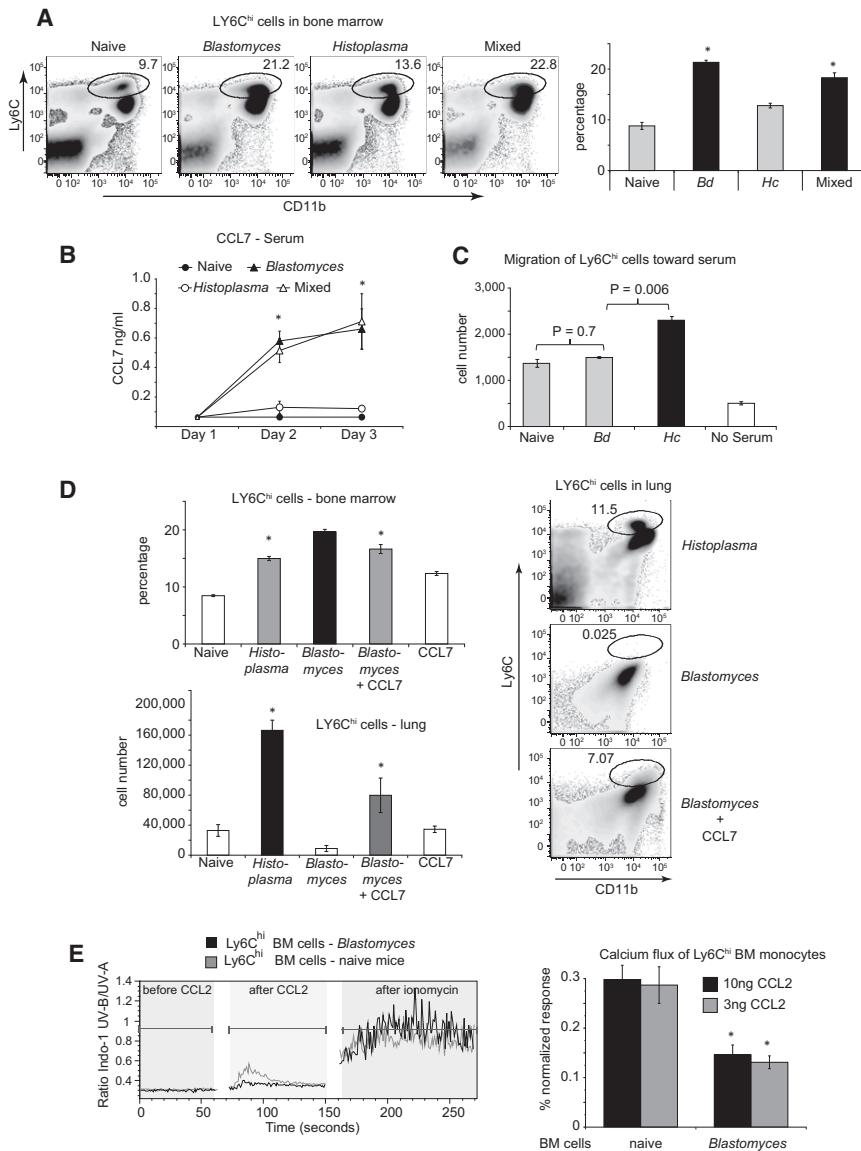


Figure 4. *B. dermatitidis* Blocks Recruitment of Ly6C^{hi} Inflammatory Monocytes to the Lung by Impairing CCL7-Induced Egress of CCR2⁺ Cells from the Bone Marrow

(A) Percentage of Ly6C^{hi} CD11b⁺ cells in the bone marrow 3 days after wild-type mice received i.t. inoculation of *Bd* (10⁵ yeast), *Hc* (10⁶), or both mixed together. Dot plots (left side) are representative of five mice per group. Histogram (right) shows the mean ± SD for each group. Data are representative of three experiments. *p < 0.05 versus *Hc* group.

(B) CCL7 levels in the serum of mice vaccinated as in (A). Results are the mean ± SD of 5 mice per group. *p < 0.05 versus *Hc* group.

(C) Ly6C^{hi} CD11b⁺ enriched cells from the bone marrow of naive mice were placed in the upper chamber of a 24-well transwell plate. The bottom chamber contains pooled serum from each group (n = 5 mice per group) at 1:2 dilution in RPMI or no serum as a control. The number of cells that migrated into the bottom chamber was counted after 6 hr of incubation. Error bars represent mean ± SD of three replicates per group; results are representative of three independent experiments.

(D) Treatment with CCL7 promotes egress of Ly6C^{hi} monocytes from the bone marrow and into the lungs of mice after vaccination with *Bd*. Mice were vaccinated with yeast by the respiratory route as in (A). Mice received CCL7 i.v. (200 ng/dose) twice a day on days 1 and 2 before analysis on day 3. Results represent the mean ± SD of five mice per group (data are representative of two independent experiments).

(E) Bone marrow cells from naive mice or *Bd*-vaccinated mice harvested 4 days later were loaded with Indo-1 and stimulated with CCL2. Free [Ca²⁺]_i was measured in monocytes by flow cytometry and gating on CD11b⁺ and Ly6C^{hi} cells (panels on left). Ionomycin was used as a positive control for maximal Ca²⁺ influx. Data are representative of four mice per group and three experiments. Results are expressed as percentage of the normalized response (right panel) and calculated as follows: [(mean of Indo-1 UV-B/UV-A ratio

after chemokine (green shading)] – [mean of Indo-1 UV-B/UV-A ratio before chemokine (pink shading)] / [(mean of Indo-1 UV-B/UV-A ratio during the response to ionomycin (blue shading)] – [mean of Indo-1 UV-B/UV-A ratio, before chemokine addition (pink shading)]. Mean and SEM values were calculated for each group and illustrated by histogram. Data are representative of three experiments.

i.t., compared to *Hc* (Figure 6B). In the *Ccr2*^{-/-} mice, 1807 cells again failed to expand in response to *Bd*. Slightly higher numbers of 1807 cells expanded in response to *Hc* in *Ccr2*^{-/-} versus wild-type mice, but the difference was insignificant. However, the differentiation of IFN γ producing Th1 1807 cells in response to *Hc* was sharply impaired in *Ccr2*^{-/-} mice in the MLN (Figures 6C and 6D), and especially after these T cells exited the nodes and migrated back into the lung (Figures 6F and 6G). In addition to impairing the differentiation of 1807 into Th1 cells, the loss of CCR2 changed the ratio of cytokine producing 1807 cells in favor of T13 and T17 cells in response to *Hc* (Figure 6G). Thus, the loss of CCR2⁺ Ly6C^{hi} CD11b⁺ DCs, due to *Bd* or CCR2 deletion, curtails activation, proliferation and Th1 differentiation of 1807 cells in the MLN and lung.

Transfer of Ly6C^{hi} CD11b⁺ CD11c⁺ DCs Enables *Bd* to Prime T Cells in the Lung

We tested whether resupply of Ly6C^{hi} CD11b⁺ CD11c⁺ DCs into the lungs restored priming of *Bd* 1807 cells. We first established conditions that lead to optimal recruitment after i.t. delivery of *Hc*. These cells peaked by day 4 in the lung and day 7 in the MLNs (Figures S6A and S6B). We collected Ly6C^{hi} monocytes from mice 7 days after exposure to *Hc*. We enriched the cells by negative selection (Figure S6C), after which Ly6C^{hi} monocytes constituted \approx 15% of the population (10- to 15-fold enrichment) and Ly6C⁺ cells made up \approx 85%. Approximately 1% to 2% of the Ly6C^{hi} monocytes harbored PKH26⁺ yeast (data not shown). We transferred the Ly6C-enriched cells i.t. into *Ccr2*^{-/-} or wild-type mice and also delivered *Bd* or *Hc* by this route

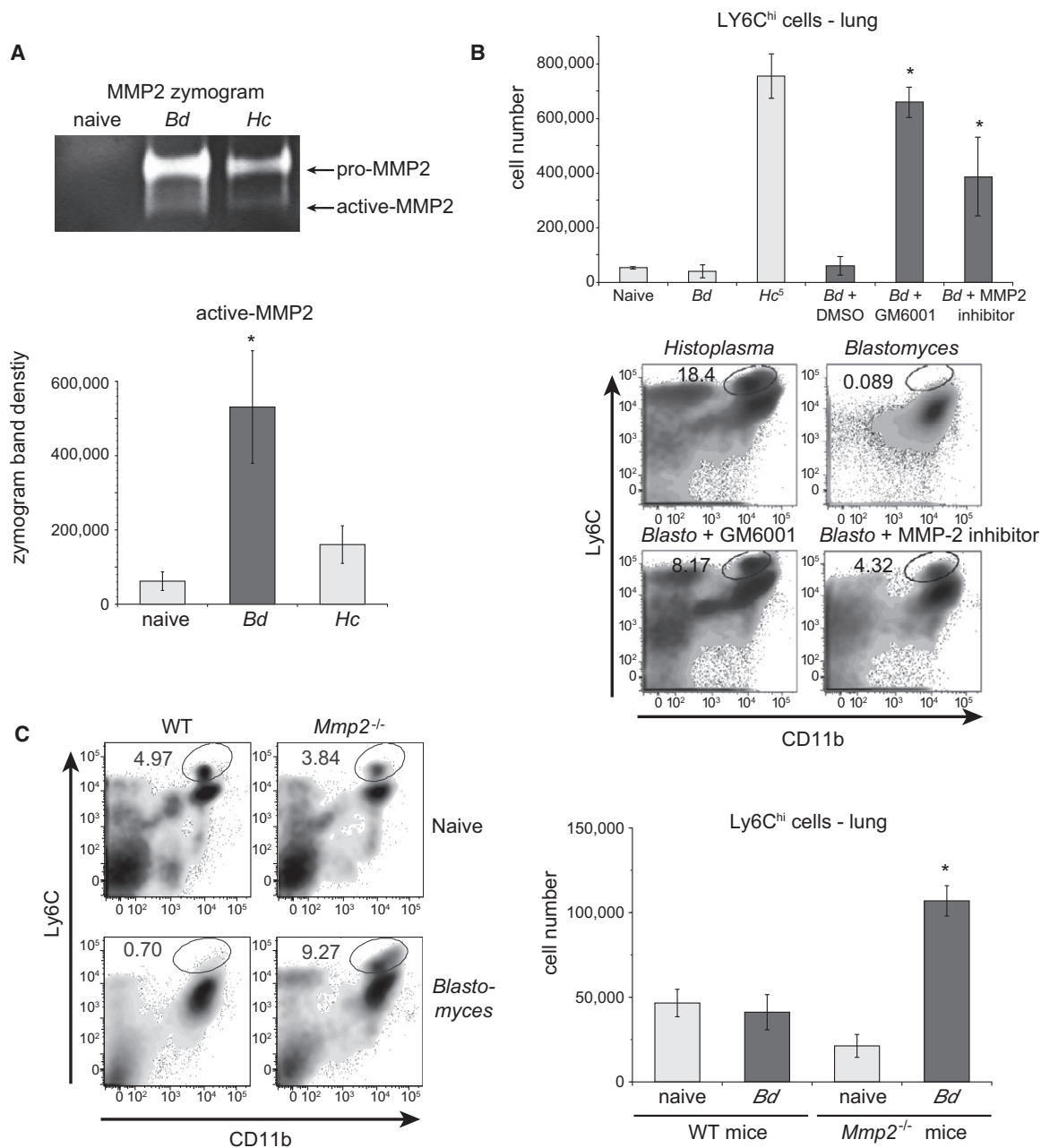


Figure 5. MMP2 Retards Recruitment of Ly6c^{high} Inflammatory Monocytes to the Lungs of Mice Vaccinated at the Respiratory Mucosa with Attenuated *Bd*

(A) Lung MMP2 levels. Mice were inoculated i.t. with 10⁵ *Bd* or 10⁶ *Hc* and lung MMP2 levels were assessed by zymography. The zymogram (upper panel) shows pro- and active MMP2 in BAL samples pooled for 5 mice/group 3 days after vaccination. The histogram shows densitometry quantification of active MMP2. Results are the mean ± SE of pixel intensity for mice (n = 5) in each group. *p < 0.05 versus *Hc*. Results are representative of 3 independent experiments.

(B) Inhibition of MMP2 promotes egress of Ly6c^{hi} monocytes from the marrow and recruitment to the lung. Mice were inoculated i.t. with *Hc* or *Bd* as above either with or without DMSO, GM6001 or MMP-2 inhibitor. On day 3, the percentage of Ly6c^{hi} monocytes in the lung (lower panels) and the number (upper panel) was determined by flow cytometry. Data are the mean ± SD of 7–10 mice/group from two independent experiments. *p < 0.05 for *Bd* groups that received DMSO alone versus GM6001 or MMP-2 inhibitors.

(C) *Mmp2*^{-/-} mice show increased recruitment of Ly6c^{hi} monocytes into the lungs. *Mmp2*^{-/-} and wild-type mice were vaccinated with *Bd* (i.t.) or not as above and four days later the percentage of Ly6c^{hi} monocytes in the lung (left panels) and the number (right panel) was determined by FACS. Data is representative of 4–5 mice/group and three independent experiments. *p < 0.05 versus all other groups.

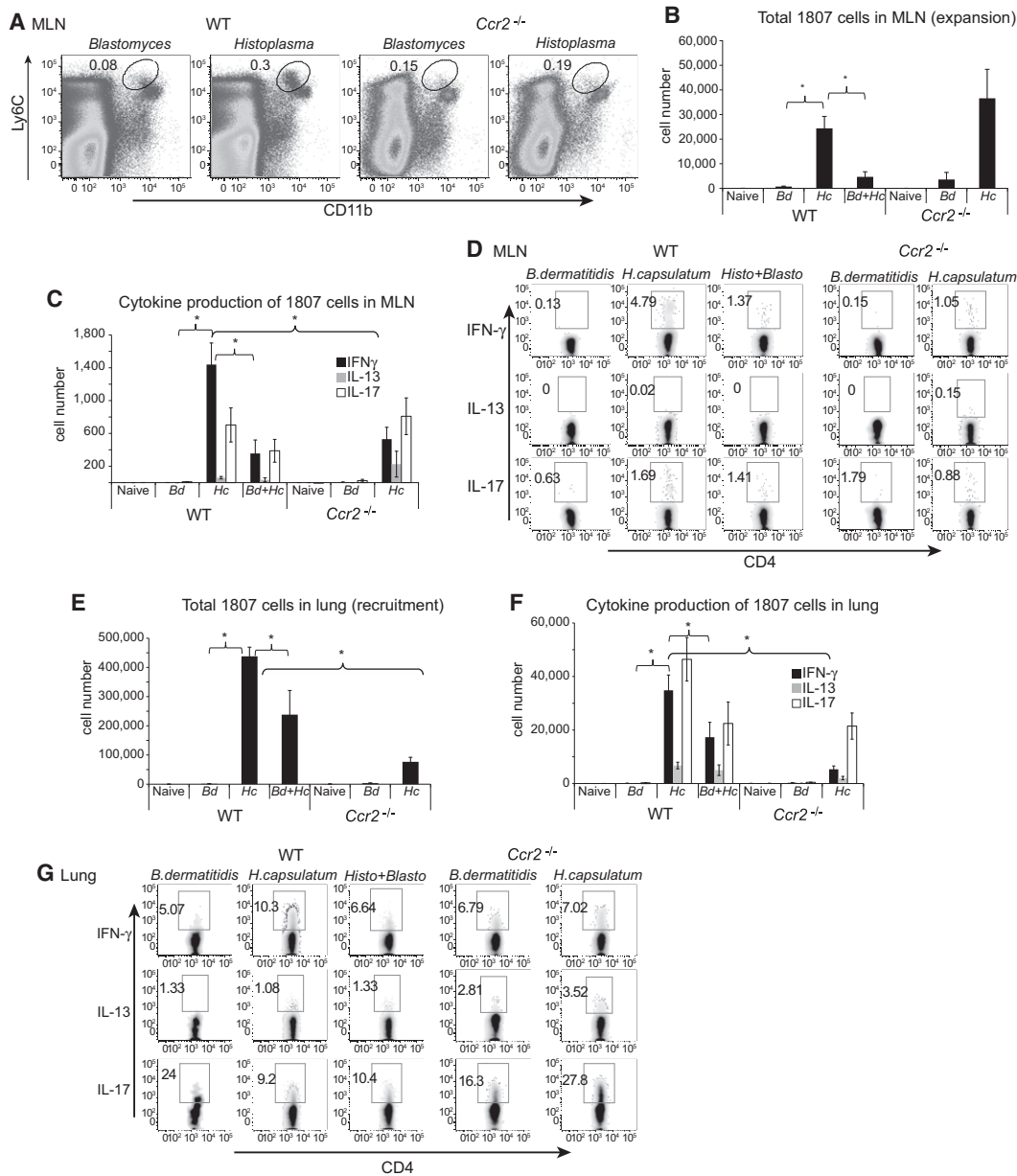


Figure 6. The Absence of Inflammatory Monocytes Curtails Activation CD4 T Cells in the Lung-Draining LNs and Their Th1 Cell Differentiation There and in the Lung

(A) Recruitment of Ly6C^{hi} monocytes (circled) into draining MLN of wild-type mice or *Ccr2*^{-/-} mice 4 days after i.t. vaccination.

(B) Expansion of *Bd* 1807 tg cells in the MLNs of wild-type or *Ccr2*^{-/-} mice that received *Bd* (10⁵), *H. capsulatum* (10⁶) or both. One day before infection, 10⁶ 1807 Thy1.1⁺ cells were transferred into Thy1.2⁺ mice. MLN were harvested 9 days post-infection. Numbers were calculated based upon FACS percentage of Thy1.1⁺ cells in MLN. Error bars are the mean ± SD of 4-5 mice/group. *p < 0.05 for comparisons indicated by brackets. Data is representative of 2 independent experiments. WT, wild-type.

(C and D) Number of IFN-γ (black bar), IL-13- (gray bar), IL-17- (white bar) producing 1807 cells in the MLNs of WT and *Ccr2*^{-/-} mice. Cells from MLN were cocultured overnight with irradiated splenocytes and *Bd* CW/M antigen, then stimulated for 4 hr with Golgistop at 37°C and stained for intracellular cytokines. Absolute numbers were calculated based upon FACS percentages shown in (D). Error bars indicate mean SD ± of four to five mice per group. *p < 0.05 for comparisons indicated by brackets. Data are representative of two independent experiments.

(E) Total number of 1807 T cells recruited back to the lung 9 days after i.t. inoculation of yeast. 1807 tg cells in the lung were analyzed as described in (B). Error bars are the mean ± SD of four to five mice per group. *p < 0.05 for comparisons indicated by brackets. Data are representative of two independent experiments.

(F and G) Cytokine producing 1807 T cells recruited to the lung. For intracellular cytokine staining, single-cell suspension from the lung is incubated with Golgistop, anti-CD3, and anti-CD28 for 4 hr at 37°C on the day of harvest and then stained for IFN-γ (black bar), IL-13 (gray bar), and IL-17 (white bar). Layout and data analysis are as described in (C) and (D).

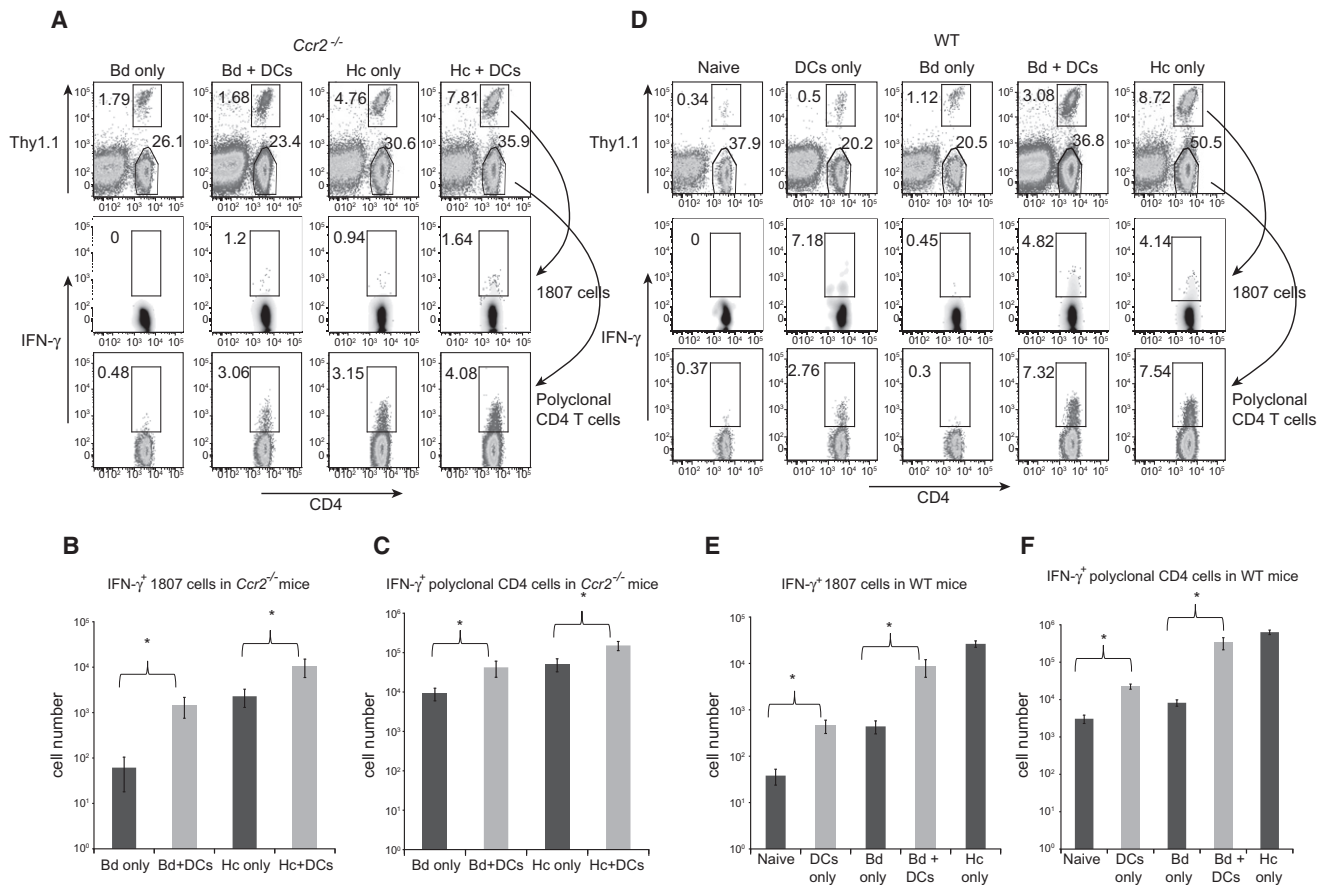


Figure 7. Adoptive Transfer of Inflammatory Monocytes into the Lung Restores the Activation and Differentiation of IFN- γ -Producing CD4⁺ T Cells in Response to *Bd*

(A and D) FACS data showing *Bd* 1807 cells in the lung of *Ccr2*^{-/-} (A) and wild-type (D) mice 10 days after injection of yeast. Transferred 1807 cells were tracked by the Thy1.1 marker (top row), and then IFN- γ production by Thy1.1 cells was intercellularly analyzed (middle row). Polyclonal CD4⁺ T cells also were analyzed for IFN- γ production by ICS (bottom row). “+DCs” indicates that the group received inflammatory DCs as indicated in (A). Groups labeled *Bd* or *Hc* received i.t. inocula of the respective yeast.

(B and C) Total number of IFN- γ -producing 1807 cells (B) or polyclonal CD4⁺ T cells (C) in *Ccr2*^{-/-} mice. Numbers were calculated on the basis of FACS percentages shown in (A). Error bars represent the mean \pm SD of four mice per group. **p* < 0.05 for comparisons indicated by brackets.

(E and F) Total number of IFN- γ -producing 1807 T cells (E) and polyclonal CD4⁺ T cells (F) in WT mice. Numbers were calculated on the basis of FACS percentages shown in (D). Error bars represent the mean \pm SD of four mice per group. **p* < 0.05 for comparisons indicated by brackets.

(Figure S6C). We verified that congenic transferred DCs persisted in the lungs over several days (Figure S6D). We analyzed the priming and differentiation of separately transferred *Bd* 1807 cells (and endogenous CD4⁺ T cells) in lungs 9 days after DC transfer.

In *Ccr2*^{-/-} mice, transfer of Ly6C^{hi} monocytes enhanced the number of IFN- γ ⁺ 1807 cells after mucosal vaccination (Figures 7A–7C): they rose \approx 100-fold in mice that received *Bd* (note *Bd* only versus *Bd* + DCs in Figure 7B) and \approx 10-fold in mice that received *Hc* (note *Hc* only versus *Hc* + DCs). Similar trends were observed among the polyclonal CD4⁺ T cells. Thus, the Ly6C^{hi} monocytes transferred into *Ccr2*^{-/-} recipients were functional and re-established activation, differentiation, and recruitment into the lungs of Th1 1807 cells.

Upon transfer into wild-type mice (Figures 7D–7F), Ly6C^{hi} monocytes exerted a similar augmentation of 1807 cell function in the lungs. Transfer of Ly6C^{hi} monocytes into unvaccinated mice enhanced the number of IFN- γ ⁺ 1807 cells, when

compared to naive mice. Transfer of these cells into mice that had been vaccinated i.t. with *Bd* had a more pronounced effect, increasing the number of IFN- γ -producing 1807 cells in the lung by nearly 100-fold (Figure 7E; note *Bd* only versus *Bd* + DCs), and the percentage of these cells by nearly 10-fold (Figure 7D; note *Bd* only versus *Bd* + DCs). Comparable trends were observed in the endogenous CD4⁺ T cell pool (Figures 7D and 7F). Thus, impaired recruitment and maturation of Ly6C^{hi} monocytes led to failed priming of CD4 T cells and skewing of their differentiation away from Th1 cells upon mucosal vaccination with *Bd*. These events were remediated by the adoptive transfer of Ly6C^{hi} monocytes.

DISCUSSION

CD4⁺ T cells that produce IFN- γ are pivotal in immunity to fungi (Cutler et al., 2007). Here, we found that respiratory mucosal vaccination with *Bd* did not prime IFN- γ -producing endogenous

CD4⁺ T cells. We used a TCR tg mouse to track Ag-specific T cells to decipher the mechanism. The host response to attenuated fungus, involving exuberant MMP and restrained inflammation, paradoxically undermined downstream priming of T cells. This finding offers a cautionary note to vaccinologists harnessing vaccine immunity at the respiratory mucosa.

Subcutaneous delivery of attenuated *Bd* recruits Ly6C^{hi} DCs to the injection site, which ferry yeast into the sDLNs (Ersland et al., 2010). Respiratory mucosal delivery of the vaccine yeast instead failed to recruit the cells. There were low numbers of these cells in the lung and MLN and few harbored yeast. *Bd* blocked recruitment and maturation of Ly6C^{hi} DCs in the lung, rather than simply failing to induce their influx and maturation. The impact of *Bd* on Ly6C^{hi} monocytes was selective. Uptake of these yeast into APCs and their trafficking into MLNs was not generally impaired, given that the number of APCs harboring *Bd* in lung and MLN was comparable to that in mice exposed to *Hc* alone or in a mixed infection. Thus, *Bd* led to a redistribution of yeast from Ly6C^{hi} monocytes, into other lung APCs.

Ly6C^{hi} monocytes regulate the early host response to *Aspergillus* lung infection by taking up conidia and trafficking them into the draining MLN to prime CD4⁺ T cells (Hohl et al., 2009). Ly6C^{hi} monocytes are dispensable in priming CD4⁺ T cells in the spleen of mice that are systemically infected i.v. with *Aspergillus*. Although Ly6C^{hi} monocytes carry *Bd* yeast into the sDLNs after s.c. vaccination (Ersland et al., 2010), in *Ccr2*^{-/-} mice lacking Ly6C^{hi} DCs, other migratory skin and resident DCs compensate by delivering yeast into the draining nodes to prime T cells. In contrast, during mucosal vaccine delivery here, the modulation of Ly6C^{hi} monocyte influx—either due to *Bd* alone or in mixed infection, or in *Ccr2*^{-/-} mice—sharply reduced the numbers of vaccine yeast delivered to the MLN and impaired priming of T cells. Thus, Ly6C^{hi} monocytes are indispensable in fungal vaccine delivery and antigen priming in the lung. *Cryptococcus neoformans* also induces the recruitment into lung of Ly6C^{hi} monocytes (Osterholzer et al., 2009), which mature into CD11b⁺ CD11c⁺ DCs, downregulate Ly6C, and promote resistance. In primary pulmonary histoplasmosis, *Ccr2*^{-/-} mice have altered leukocyte influx in their lungs and succumb to infection due to overproduction of IL-4 and alternative activation of pulmonary macrophages (Szymczak and Deepe, 2009).

Several chemokines can bind CCR2. CCL2 and CCL7 are the main CCR2 ligands in inflammatory settings (Jia et al., 2008; Tsou et al., 2007) and help mobilize monocytes from the bone marrow. Vaccination with *Bd* led to trapping of these cells in the marrow and was also associated with high levels of CCL7 in serum. The serum CCL7 in these mice was inactive, failing to promote CCR2-dependent migration of Ly6C^{hi} monocytes in chemotactic assays. Further, treatment of these vaccinated mice with rCCL7 repaired the deficit, promoting egress of CCR2⁺ cells from the marrow and entry into the lung. We propose that CCL7 was rendered inactive by MMP2 because this product was elevated in *Bd*-vaccinated mice and its inhibition relieved marrow trapping and promoted Ly6C^{hi} cell recruitment to the lung. Removal of N-terminus residues of CCL7 by MMP2 impairs its activity, yet CCL7 can still bind its receptor and compete with CCL2 (McQuibban et al., 2000; McQuibban et al., 2002). Host MMP2 may have modified CCL7 impairing

its action, perhaps also antagonizing CCL2. Inflammatory monocytes from the marrow of *Bd*-vaccinated mice showed reduced sensitivity and response to CCL2. Although these defects could be partially corrected with exogenous rCCL7, we did not measure serum CCL7 levels after treatment and cannot exclude a pharmacological effect. In hepatitis C, serum CXCL10, which recruits lymphocytes to the liver by binding surface CXCR3, is paradoxically elevated in the patients who fail therapy (Casrouge et al., 2011). Elevated levels of the protease dipeptidyl peptidase IV (DPP4) cleaves CXCL10, converting it from an agonist into an antagonist of CXCR3. Although MMP2 probably acts similarly herein, we cannot exclude a role for other MMPs including being of fungal origin.

Impaired recruitment and maturation of Ly6C^{hi} monocytes by *Bd* blunted the activation, expansion, and differentiation of IFN- γ -producing T cells in the draining MLN and profoundly altered differentiation of T cells on migration to the lungs. *Bd* 1807 cells showed deficits in these functions after respiratory mucosal vaccination with *Bd* (but not after s.c. vaccination). Because *Bd* 1807 cells recognize a shared antigen in *Bd* and *Hc*, we could show that priming and Th1 differentiation of these T cells by *Hc* is impaired not only in *Ccr2*^{-/-} mice, but also in wild-type mice upon mucosal delivery of mixed *Bd* and *Hc*. Thus, yeast modulation of Ly6C^{hi} monocytes mediates failed T cell priming after mucosal vaccination with *Bd*. We substantiated the role of Ly6C^{hi} monocytes by adoptive transfer, which restored priming, expansion, and Th1 cell differentiation of *Bd* 1807 cells. Consistent with our findings, prior reports showed that inflammatory monocyte-derived DCs stimulate Th1 immune responses. In *Ccr2*^{-/-} mice, Th1 CD4⁺ T cell responses are impaired due to reduced monocyte recruitment to inflamed LNs and diminished production of IL-12 at the time of CD4⁺ T cell priming (Nakano et al., 2009; Peters et al., 2000; Peters et al., 2001). Similarly, in pulmonary cryptococcosis, *Ccr2*^{-/-} mice redirect CD4⁺ T cell differentiation from Th1 to Th2 cells (Blease et al., 2000; Traynor et al., 2000).

Impaired recruitment and maturation of Ly6C^{hi} monocytes skewed the differentiation of *Bd* 1807 cells toward IL-13- and IL-17-producing cells. This was especially evident in the 1807 cells that had fully differentiated after migrating back to the lung in *Ccr2*^{-/-} mice that received *Hc*. This was also true for 1807 cells in mice that received mixed infection. Our findings suggest that other APCs in the lung of wild-type mice that received *Bd* or mixed infection or in the *Ccr2*^{-/-} mice that received *Hc*, promote the differentiation of CD4⁺ T cells into IL-13- and IL-17-producing cells. Szymczak and Deepe (2009) found that lung IFN- γ levels were unaltered in *Hc* infected *Ccr2*^{-/-} mice, but elevated IL-4 levels instead led to their death. IL-17 levels were not reported in that study, but it was not possible to track Ag-specific T cells to assess skewed differentiation in the LNs or lung.

Priming Ag-specific immunity at mucosal sites of pathogen entry is an active area in vaccine development. Our study highlights pitfalls in applying this strategy broadly across pathogen kingdoms. There are four commercially available mucosal vaccines: polio, rotavirus, *Salmonella typhi*, and influenza—each a live, attenuated vaccine. HIV vaccine development is focused on strategies for a mucosal vaccine. Intranasal vaccine delivery of respiratory viruses is thought to prime immunity in nasal mucosa-associated lymphoreticular tissue, and engage

not only s-IGA, but also T cell immunity, particularly CTLs. Persistent antigen in the lung after influenza A infection fosters antigen uptake by specialized respiratory DC that prime memory T cells (Kim et al., 2010). Although CCR2⁺ cells govern resistance to *M. tuberculosis* (Peters et al., 2001), enhanced recruitment of inflammatory monocytes to the lungs of mice infected with *M. tuberculosis* with intranasal poly-IC unexpectedly enhanced pathogen growth in this permissive population and lung tissue injury despite unaltered production of IFN- γ (Antonelli et al., 2010).

These studies illustrate differences among pathogen kingdoms in vaccine or therapeutic strategies targeted to respiratory sites of pathogen entry. Our work sheds new light on this variability by highlighting the role of chemokines and their cellular targets in inducing mucosal immunity and by unveiling the paradoxical effect of the host in undermining immunity to a mucosal vaccine. To optimize the efficacy of mucosal vaccination, suitable vaccine adjuvants may thus need to target host MMP responses that counter adaptive immunity at the lung mucosa.

Targeted recruitment of leukocytes to the lung on vaccination may augment vaccine strategies.

EXPERIMENTAL PROCEDURES

Fungi

Bd strain 55, *Hc* strain G217B and *C. albicans* strain SC5314 were previously described (Brandhorst et al., 1999). For a detailed description, see Supplemental Experimental Procedures.

Mice

The generation and characterization of *Bd* 1807 mice is described in detail in the accompanying Supplemental Experimental Procedures.

Desensitization Studies

For measuring monocyte migration in response to serum or chemokine, bone marrow cells were enriched for Ly6C^{hi}CD11b⁺ cells, placed in the upper chamber of transwell plates, and allowed to migrate through the trans-membrane. For Ca²⁺-flux measurement, monocytes were loaded with Indo-1 and stimulated with chemokine, and the flux was recorded over time by flow cytometry. For a detailed description, see Supplemental Experimental Procedures.

SUPPLEMENTAL INFORMATION

Supplemental Information includes six figures and Supplemental Experimental Procedures (including adoptive transfer of *Bd* 1807 cells, vaccination and experimental infection, PKH26 staining of yeast, lung and mediastinal LN preparation, flow cytometry, adoptive transfer of inflammatory monocytes, generation of bone marrow dendritic cells, zymography, chemokine analysis and administration of recombinant CCL7 into mice, chemotaxis assay, calcium flux measurements, in vivo treatment with MMP2 inhibitors, and statistics) and can be found with this article online at doi:10.1016/j.immuni.2012.02.015.

ACKNOWLEDGMENTS

This work was supported by grants from the USPHS to B.K. and M.W. We thank A. Starr and C. Overall from the University of British Columbia, Canada, for providing advice on the MMP2 assays and R. Gordon from the department of Pediatrics at the University of Wisconsin for assistance with illustrations.

Received: September 30, 2010

Revised: December 30, 2011

Accepted: February 2, 2012

Published online: April 5, 2012

REFERENCES

- Ali, S., Robertson, H., Wain, J.H., Isaacs, J.D., Malik, G., and Kirby, J.A. (2005). A non-glycosaminoglycan-binding variant of CC chemokine ligand 7 (monocyte chemoattractant protein-3) antagonizes chemokine-mediated inflammation. *J. Immunol.* *175*, 1257–1266.
- Antonelli, L.R., Gigliotti Rothfuchs, A., Gonçalves, R., Roffé, E., Cheever, A.W., Bafica, A., Salazar, A.M., Feng, C.G., and Sher, A. (2010). Intranasal Poly-IC treatment exacerbates tuberculosis in mice through the pulmonary recruitment of a pathogen-permissive monocyte/macrophage population. *J. Clin. Invest.* *120*, 1674–1682.
- Blease, K., Mehrad, B., Standiford, T.J., Lukacs, N.W., Gosling, J., Boring, L., Charo, I.F., Kunkel, S.L., and Hogaboam, C.M. (2000). Enhanced pulmonary allergic responses to *Aspergillus* in CCR2^{-/-} mice. *J. Immunol.* *165*, 2603–2611.
- Brandhorst, T.T., Wüthrich, M., Warner, T., and Klein, B. (1999). Targeted gene disruption reveals an adhesin indispensable for pathogenicity of *Blastomyces dermatitidis*. *J. Exp. Med.* *189*, 1207–1216.
- Brown, G.D. (2011). Innate antifungal immunity: the key role of phagocytes. *Annu. Rev. Immunol.* *29*, 1–21.
- Casrouge, A., Decalf, J., Ahloulay, M., Lababidi, C., Mansour, H., Vallet-Pichard, A., Mallet, V., Mottez, E., Mapes, J., Fontanet, A., et al. (2011). Evidence for an antagonist form of the chemokine CXCL10 in patients chronically infected with HCV. *J. Clin. Invest.* *121*, 308–317.
- Cutler, J.E., Deepe, G.S., Jr., and Klein, B.S. (2007). Advances in combating fungal diseases: vaccines on the threshold. *Nat. Rev. Microbiol.* *5*, 13–28.
- Deepe, G.S., Jr., and Seder, R.A. (1998). Molecular and cellular determinants of immunity to *Histoplasma capsulatum*. *Res. Immunol.* *149*, 397–406.
- Ersland, K., Wüthrich, M., and Klein, B.S. (2010). Dynamic interplay among monocyte-derived, dermal, and resident lymph node dendritic cells during the generation of vaccine immunity to fungi. *Cell Host Microbe* *7*, 474–487.
- Hohl, T.M., Rivera, A., Lipuma, L., Gallegos, A., Shi, C., Mack, M., and Pamer, E.G. (2009). Inflammatory monocytes facilitate adaptive CD4 T cell responses during respiratory fungal infection. *Cell Host Microbe* *6*, 470–481.
- Jia, T., Serbina, N.V., Brandl, K., Zhong, M.X., Leiner, I.M., Charo, I.F., and Pamer, E.G. (2008). Additive roles for MCP-1 and MCP-3 in CCR2-mediated recruitment of inflammatory monocytes during *Listeria monocytogenes* infection. *J. Immunol.* *180*, 6846–6853.
- Kim, T.S., Hufford, M.M., Sun, J., Fu, Y.X., and Braciale, T.J. (2010). Antigen persistence and the control of local T cell memory by migrant respiratory dendritic cells after acute virus infection. *J. Exp. Med.* *207*, 1161–1172.
- Lambrech, B.N., and Hammad, H. (2009). Biology of lung dendritic cells at the origin of asthma. *Immunity* *31*, 412–424.
- McQuibban, G.A., Gong, J.H., Tam, E.M., McCulloch, C.A., Clark-Lewis, I., and Overall, C.M. (2000). Inflammation dampened by gelatinase A cleavage of monocyte chemoattractant protein-3. *Science* *289*, 1202–1206.
- McQuibban, G.A., Gong, J.H., Wong, J.P., Wallace, J.L., Clark-Lewis, I., and Overall, C.M. (2002). Matrix metalloproteinase processing of monocyte chemoattractant proteins generates CC chemokine receptor antagonists with anti-inflammatory properties in vivo. *Blood* *100*, 1160–1167.
- Nakano, H., Lin, K.L., Yanagita, M., Charbonneau, C., Cook, D.N., Kakiuchi, T., and Gunn, M.D. (2009). Blood-derived inflammatory dendritic cells in lymph nodes stimulate acute T helper type 1 immune responses. *Nat. Immunol.* *10*, 394–402.
- Osterholzer, J.J., Chen, G.H., Olszewski, M.A., Curtis, J.L., Huffnagle, G.B., and Toews, G.B. (2009). Accumulation of CD11b⁺ lung dendritic cells in response to fungal infection results from the CCR2-mediated recruitment and differentiation of Ly-6Chigh monocytes. *J. Immunol.* *183*, 8044–8053.
- Peters, W., Dupuis, M., and Charo, I.F. (2000). A mechanism for the impaired IFN-gamma production in C-C chemokine receptor 2 (CCR2) knockout mice: role of CCR2 in linking the innate and adaptive immune responses. *J. Immunol.* *165*, 7072–7077.
- Peters, W., Scott, H.M., Chambers, H.F., Flynn, J.L., Charo, I.F., and Ernst, J.D. (2001). Chemokine receptor 2 serves an early and essential role in

- resistance to *Mycobacterium tuberculosis*. *Proc. Natl. Acad. Sci. USA* **98**, 7958–7963.
- Rivera, A., Ro, G., Van Epps, H.L., Simpson, T., Leiner, I., Sant'angelo, D.B., and Pamer, E.G. (2006). Innate Immune Activation and CD4(+) T Cell Priming during Respiratory Fungal. *Infect. Immun.* **25**, 665–675.
- Serbina, N.V., Jia, T., Hohl, T.M., and Pamer, E.G. (2008). Monocyte-mediated defense against microbial pathogens. *Annu. Rev. Immunol.* **26**, 421–452.
- Serbina, N.V., and Pamer, E.G. (2006). Monocyte emigration from bone marrow during bacterial infection requires signals mediated by chemokine receptor CCR2. *Nat. Immunol.* **7**, 311–317.
- Shi, C., and Pamer, E.G. (2011). Monocyte recruitment during infection and inflammation. *Nat. Rev. Immunol.* **11**, 762–774.
- Steinman, R.M. (2008). Dendritic cells in vivo: a key target for a new vaccine science. *Immunity* **29**, 319–324.
- Szymczak, W.A., and Deepe, G.S., Jr. (2009). The CCL7-CCL2-CCR2 axis regulates IL-4 production in lungs and fungal immunity. *J. Immunol.* **183**, 1964–1974.
- Traynor, T.R., Kuziel, W.A., Toews, G.B., and Huffnagle, G.B. (2000). CCR2 expression determines T1 versus T2 polarization during pulmonary *Cryptococcus neoformans* infection. *J. Immunol.* **164**, 2021–2027.
- Tsou, C.L., Peters, W., Si, Y., Slaymaker, S., Aslanian, A.M., Weisberg, S.P., Mack, M., and Charo, I.F. (2007). Critical roles for CCR2 and MCP-3 in monocyte mobilization from bone marrow and recruitment to inflammatory sites. *J. Clin. Invest.* **117**, 902–909.
- Vermaelen, K., and Pauwels, R. (2004). Accurate and simple discrimination of mouse pulmonary dendritic cell and macrophage populations by flow cytometry: methodology and new insights. *Cytometry A* **67**, 170–177.
- Wüthrich, M., Deepe, G., and Klein, B. (2012). Adaptive Immunity to Fungi. *Annu. Rev. Immunol.* Published online January 3, 2012.
- Wüthrich, M., Filutowicz, H.I., Allen, H.L., Deepe, G.S., and Klein, B.S. (2007). V beta1+ J beta1.1+V alpha2+ J alpha49+ CD4+ T cells mediate resistance against infection with *Blastomyces dermatitidis*. *Infect. Immun.* **75**, 193–200.
- Wüthrich, M., Filutowicz, H.I., and Klein, B.S. (2000). Mutation of the WI-1 gene yields an attenuated *blastomyces dermatitidis* strain that induces host resistance. *J. Clin. Invest.* **106**, 1381–1389.
- Wüthrich, M., Hung, C.Y., Gern, B.H., Pick-Jacobs, J.C., Galles, K.J., Filutowicz, H.I., Cole, G.T., and Klein, B.S. (2011b). A TCR transgenic mouse reactive with multiple systemic dimorphic fungi. *J. Immunol.* **187**, 1421–1431.